ELSEVIER

Journal of Nuclear Materials 303 (2002) 169–176

journal of nuclear materials

www.elsevier.com/locate/jnucmat

Effect of the circumferential hydrides on the deformation and fracture of Zircaloy cladding tubes

S.I. Hong [a,*], K.W. Lee [a], K.T. Kim [b]

[a] *Department of Metallurgical Engineering, Solidified Materials Research Center, Chungnam National University, Taedok Science Town, Taejon 305-764, South Korea*

[b] *Research and Development Center, KEPCO Nuclear Fuel Co. Ltd., Taejon 305-303, South Korea*

Received 6 July 2001; accepted 22 February 2002

Abstract

The hydride formation and its effect on the deformation and fracture of two different types of Zircaloy cladding tubes were investigated. The effect of cooling rate on the size and distribution of hydrides were also examined. Hydrides were more homogeneously distributed with high cooling rate (i.e., air-cooled) and clustered with low cooling rate (i.e., furnace-cooled). The room temperature strength increased slightly and the ductility decreased with the formation of the hydrides. The mechanical properties were slightly modified by the size and distribution of hydrides. Secondary cracks along the platelets of hydrides were observed on the fracture surfaces of tubes. The slight loss of ductility in the presence of circumferential hydrides is thought to be associated with the secondary cracking during the final process of the fracture. The deformation behavior of the tubes was not greatly influenced by the presence of the circumferential hydrides. The rate controlling mechanism of the deformation can be explained by the dislocation intersection mechanism in which the segregation of alloying elements on dislocations affects the activation length. © 2002 Published by Elsevier Science B.V.

1. Introduction

Zirconium and its alloys have been used for many years in chemical and nuclear engineering applications involving severe combinations of temperature and reactive environments [1,2]. Zircaloy-4, one of the zirconium alloys, has satisfactory mechanical strength [3–6] and corrosion resistance to nitric acid and hydrochloric acid [7,8]. When the alloy is used in a nuclear reactor, its hydride is necessarily formed from external hydrogen sources such as waterside corrosion, dissolved hydrogen in coolant water and water radiolysis, and internal sources such as hydrogen content in fuel pellets and moisture absorbed by the uranium dioxide fuel pellet [9].

The precipitation of hydride in the Zircaloy-4 cladding tube results in embrittlement of the tubing. The extent of hydride embrittlement depends not only on the quantity of hydride present, but also on its morphology and in particular the orientation of hydrides with respect to the applied stress [10]. For a tubular component internally pressurized in service, it is desirable to have the hydride platelets oriented with their major axis in the circumferential direction. Hydride orientation is to a large extent determined by the manufacturing process, which has a great influence on the texture and the shape and size of grains [10]. Cold tube reduction process (pilgering), which is used in the fabrication of cladding tubes, fortunately produces material with a strong tendency to form circumferentially oriented hydrides. In this study, the hydride formation characteristic and its

* Corresponding author. Tel.: +82-42 821 6595; fax: +82-42 822 9401.

E-mail address: sihong@cnu.ac.kr (S.I. Hong).

0022-3115/02/$ - see front matter © 2002 Published by Elsevier Science B.V.
PII: S0022-3115(02)00814-0

effect on the mechanical properties in two different commercial cladding tubes were studied.

2. Experimental procedure

Two different types of Zircaloy-4 tubes used in this study were supplied by the Korea Nuclear Fuel Company. One is the regular stress-relieved Zircaloy-4 tubes with the basal poles oriented at about 30° from the tube radial direction [6]. The other is the stress-relieved Zircaloy-4 tubes with 1 mm thick low-tin Zircaloy layer on the outer surface. The dimensions of tubes are shown in Fig. 1. The regular Zircaloy-4 tubes will be called R-type (Zircaloy (R)) and the tubes with the outer layer will be called L-type (Zircaloy (L)) hereafter. The chemical compositions are given in Table 1. As shown in the table, the outer layer of the L-type tubes contains a lower Sn content than the regular Zircaloy-4. The Corrosion resistance was reported to be improved markedly by decreasing the Sn content from the specification range of Zircaloy-4 to 0.65% [11,12]. The outer layer of L-type tubes is expected to exhibit excellent waterside corrosion properties.

The tubes were charged with hydrogen using the high temperature cathodic hydrogen charging method [8].

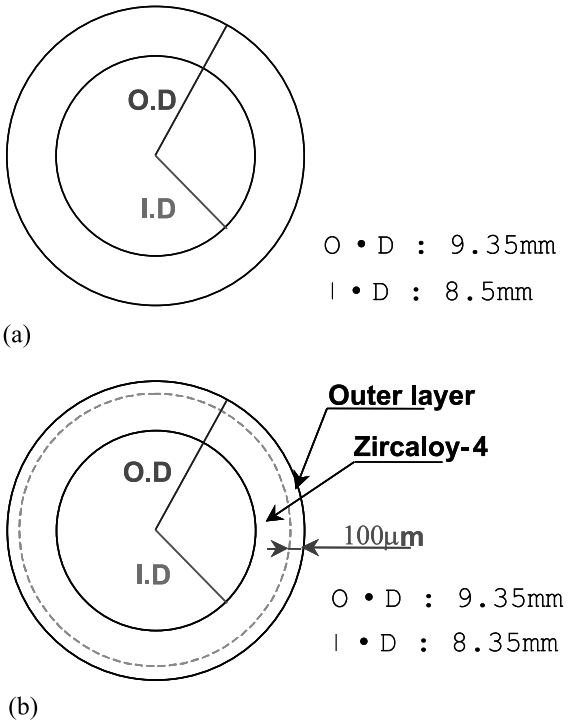

Fig. 1. Dimensions and shapes of the transverse sections of R-type (a) and L-type (b) tubes.

Table 1
Chemical compositions of R-type and L-type Zircaloy tubes

		Sn	Fe	Cr	O	Zr
L-type	Outer layer	0.81	0.28	0.16	0.13	Bal.
	Zircaloy-4	1.47	0.21	0.10	0.14	Bal.
R-type		1.34	0.22	0.11	0.13	Bal.

Fig. 2 is a schematic of hydrogen-charging experimental apparatus. The chemistry of the electrolyte solution is shown in Table 2. A direct current was supplied galvanostatically to the working electrode, Zircaloy specimens, and a counter electrode at 0.2–0.5 A/cm^2. The counter electrode was a graphite tube. Since the decomposition of water in the NaOH and sulphate/bisulphate salt system is the preferred reaction for the temperature above the 80 °C, the electrolysis of water in a container can liberate hydrogen [13]. During the charging process, the voltage change between reference electrode and working electrode was recorded.

When the electrochemically evolved hydrogen ions are applied to the Zircaloy-4 working electrode, a part of the absorbed ions diffuses into the alloy and the other part is liberated from the surface as a hydrogen gas. The volume of the gaseous hydrogen is measured by an attached burette, which is converted to the number of hydrogen ions by the ideal gas equation [8]. The hydrogen content was measured to be 1260 ppm [8]. In order to stabilize hydrogen in the specimens as hydride form, vacuum annealing was carried out at 400 °C for 3 h after chemically cleaning of the specimen surface with acetic acid. After annealing, the tubes were cooled either in furnace or in air to investigate the effect of cooling rate on the hydride morphologies. The cooling rates for furnace cooling and air cooling were approximately 4 °C/s and 126 °C/s, respectively. The morphology of hydrides was observed with an optical microscope after etching.

The strength and ductility were measured using the ring tensile test to investigate the circumferential properties. Ring specimens with the width of 4 mm were cut transversely from the cladding tube and tension tested using a special grip. Fig. 3 shows the schematic configuration of the ring specimen and two half-cylinders that open and strain the ring specimen. As shown in this figure, 0.7 mm wide space was given between two half-cylinders to allow free plastic flow at the beginning of the tensile test. The diameter of the half-cylinders in Fig. 3 was 8.35 mm. Tensile testing was performed using a united testing machine (SFP 10) at room temperature. The gage length for the calculation of strain rate was assumed to be 5 mm. The detailed explanation on the determination of the gage length was given in Ref. [6]. The fracture surfaces were examined using a JEOL-6400 scanning electron microscope.

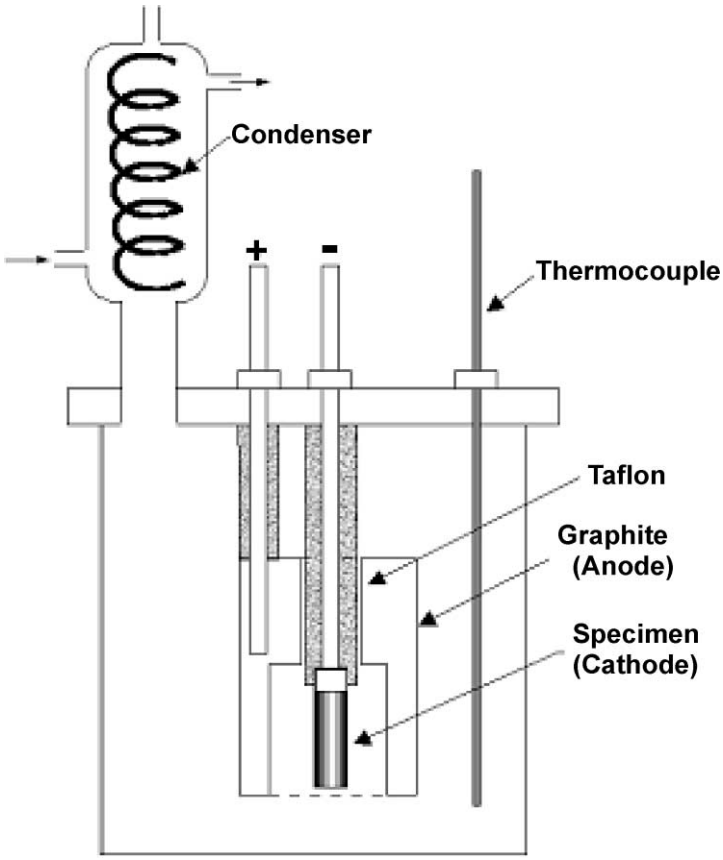

Fig. 2. Schematic diagram of hydrogen-charging apparatus.

Table 2
Chemistry of electrolyte solution

Electrolyte	$NaHSO_4 + H_2O = 1000{:}300$
Temperature	125 °C
Current density	0.3 A/cm^2
Time	24 h

3. Results and discussion

Fig. 4 shows the three-dimensional (3D) views of R-type Zircaloy tubes and L-type Zircaloy tubes with the outer layer after hydriding by a high temperature cathodic charging method, followed by annealing at 400 °C for 3 h. Both intergranular and intragranular hydride precipitates have grown circumferentially [8]. The distribution and size of hydrides were greatly influenced by the cooling rate. Hydride platelets were rather homogeneously distributed in air-cooled tubes (Fig. 4(a) and (c)) whereas they were grouped into long bands in furnace-cooled tubes (Fig. 4(b) and (d)). The distribution, size and shape of hydride platelets in the outer layer of L-type Zircaloy tubes (Fig. 4(c)) were quite similar to

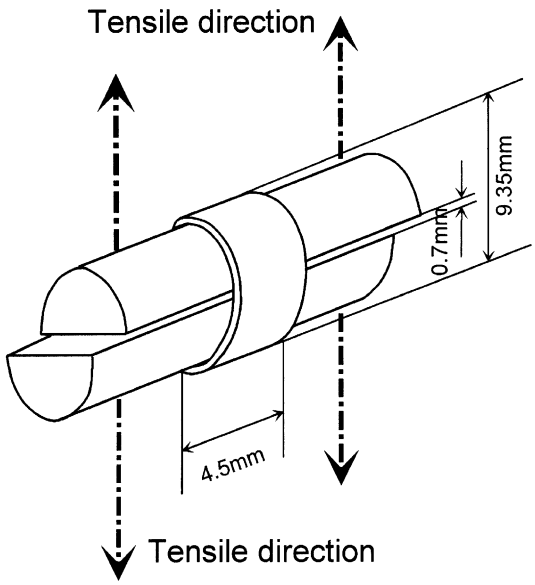

Fig. 3. Schematic configuration of tensile testing sample and grip.

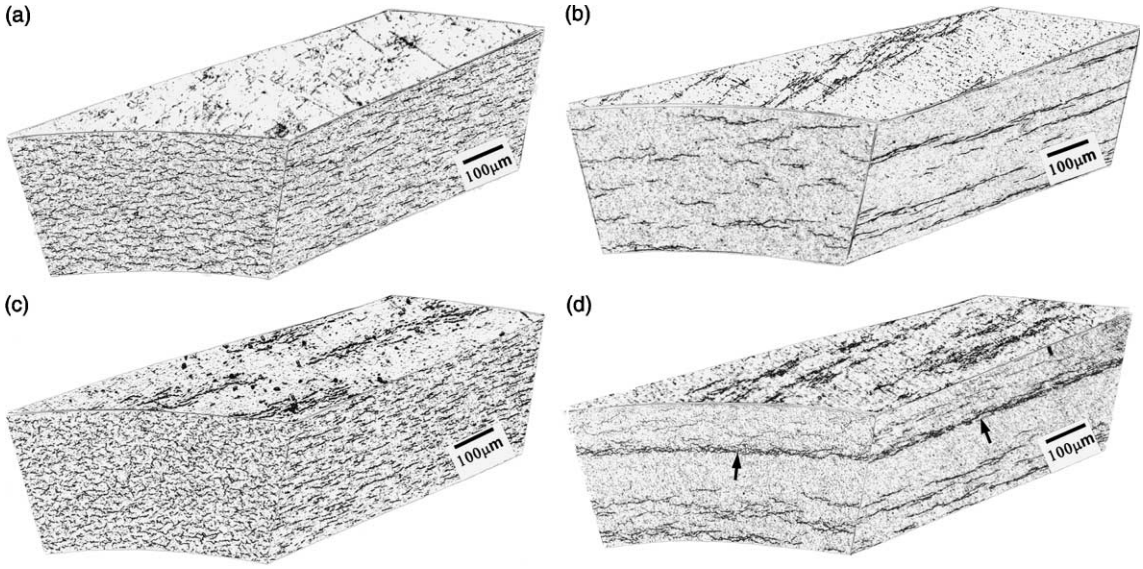

Fig. 4. 3D views of R-type (a, b) and L-type (c, d) Zircaloy tubes with hydrides. Air cooled (a, c) and furnace-cooled (b, d).

those in the Zircaloy-4 matrix after air-cooling. The distribution of hydrides, however, was significantly modified in furnace-cooled L-type tubes. As seen in Fig. 4(d), hydrides preferentially precipitated along the interface (indicated by an arrow) between the outer layer and the matrix when furnace-cooled. It should be noted that a hydride-poor region was observed just beneath the hydride-rich interface, suggesting hydrogen was depleted in near-interface regions. Hydride clustering in furnace-cooling is associated with a low nucleation rate of hydrides and high diffusivity at higher temperatures.

Fig. 5 shows the stress–strain responses of as-received (non-hydrided) and hydrided (air-cooled and furnace-cooled) Zircaloy tubes. The strength increased slightly whereas the ductility decreased after hydriding. The increase of strength suggests that the circumferential hydride does not act as a fatal crack-initiating site. Rather, the Zircaloy tubes can be slightly strengthened by circumferential hydrides [14,15]. However, the ductility decreased slightly after the formation of circumferential hydrides. In both R-type and L-type tubes, the ductility of air-cooled tubes is greater than that of furnace-cooled tubes, implying that the segregated long hydrides is more detrimental to the ductility although they were circumferentially oriented.

Fig. 6 shows the fracture surfaces of as-received (a, d) and hydrided (b, c, e, f) R-type (a, b, c) and L-type (d, e, f) Zircaloy tubes. Both non-hydrided and hydrided tubes exhibited ductile fracture behavior although the secondary cracks along the Zircaloy platelets are clearly visible in hydrided tubes. The length of secondary cracks (20–30 μm) in air-cooled Zircaloy (Fig. 6(b) and (e)) with hydrides is close to the length of hydride platelets. The secondary cracks in the furnace-cooled tubes (Fig. 6(c) and (f)) are much longer and deeper, reflecting the grouping of hydrides into bands. It is interesting to note that, in furnace-cooled L-type tubes (Fig. 6(f)), a large secondary crack (marked with an arrow) was formed along the interface between the outer layer and the matrix where the hydrides were segregated. It should also be noted that another relatively large secondary crack (marked with a double arrow) was formed about 100 μm below the interface crack. The secondary crack marked with a double arrow appears to be formed at the lower bound of the hydride-poor region. This suggestion is supported by the observation in Fig. 4(b) that the hydride-poor region beneath the hydride-rich interface extends up to 100 μm.

Fig. 7 shows the transverse sections of the air-cooled (a) and furnace-cooled (b) L-type tubes after fracture, which clearly shows that secondary cracks are associated with the hydride platelets. In Fig. 7(b), relatively deep secondary cracks are clearly visible at the interface between the outer layer and the matrix (marked with an arrow) and at the lower bound (marked with a double arrow) of the hydride-poor region.

In order to investigate the deformation mechanism of Zircaloy tubes, the activation volume for plastic flow was measured. The activation volume associated with the deformation process has been obtained from the following classical equation [16]:

$$V_{\text{app}} = kT\frac{\partial \ln \dot{\gamma}}{\partial \tau} \cong kT\frac{\ln(\dot{\varepsilon}_1/\dot{\varepsilon}_2)}{\tau_1 - \tau_2}, \tag{1}$$

where k is the Boltzmann's constant, $\dot{\gamma}$ is the shear strain rate, τ_1 and τ_2 are the applied shear stresses at the nor-

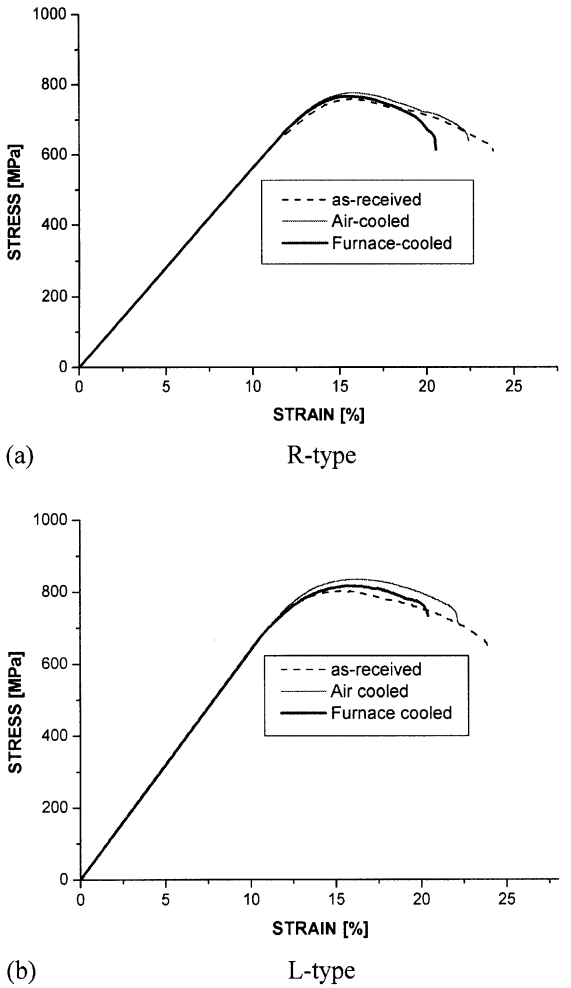

Fig. 5. Stress–strain responses of non-hydrided and hydrided Zircaloy tubes.

mal strain rates ε_1 and ε_2 and T is the absolute temperature. The shear stress τ was calculated from the yield stress σ_y, using the relation $\tau = \sigma_y/m$, where m is the Taylor factor. According to Luton and Jonas, m is assumed to be equal to 4 [17]. The calculated apparent activation volumes were 35–46b^3 (where b is the Burgers vector) for as-received (non-hydrided) R-type Zircaloy-4 tubes, and 30–41b^3 for air-cooled R-type Zircaloy-4 tubes.

Since there is no significant difference in the value of the activation volumes before and after hydride formation, the deformation mechanism is not appreciably modified by the presence of circumferential hydrides. The similarity of the stress–strain curves before and after hydride formation in Fig. 5 strongly supports that circumferential hydrides have no appreciable effect on the deformation behavior. The circumferential hydrides of the length of approximately 10 μm spaced or more are not likely the rate-controlling obstacles during plastic deformation of Zircaloy-4 tubes. This suggestion is consistent with the observation of Hong et al. [18,19] that the activation volume and the rate-controlling mechanism of Al matrix composites reinforced with 10–20 μm ceramic particles are not greatly influenced by the presence of ceramics.

The basic rate-controlling mechanisms that could be operative in zirconium alloys are

(1) intersection of dislocations ($V^* = 10^3$–$10^4 b^3$ when the dislocation density is lower than 109 cm^{-2}, $V^* < 10^2 b^3$ when the dislocation density is higher than 10^{11} cm^{-2}),
(2) Peierls–Nabarro force ($V^* = 10$–$10^2 b^3$),
(3) non-conservative motion of jogs ($V^* = 10^2$–$10^4 b^3$),
(4) cross-slip ($V^* = 10$–$10^2 b^3$ depending on stacking fault energy),
(5) overcoming of oxygen atoms by dislocation ($V^* = 1$–$10^3 b^3$ depending on the concentration of oxygen atoms).

Hong et al. [3] investigated the thermally activated deformation of annealed Zircaloy-4 and found that the activation volume was 200–300b^3 at room temperature. Since the Zircaloy tubes in this study was stress-relieved, the microstructural scale of tubes in the present study is much finer than that of annealed Zircaloy-4, which may be responsible for the smaller activation volume in the present study. The possible rate-controlling mechanism of zirconium alloys, therefore, could explain the dependence of the activation volume on the microstructural scale dependent on the deformation processing.

The Peierls–Nabarro force can be eliminated as possible rate-controlling mechanism since the Peierls–Nabarro force is not dependent on the deformation processing history. Cross-slip can also be eliminated as possible rate-controlling mechanism since the cross-slip does not occur easily in hcp metals and the magnitude of the activation volume due to cross-slip is not dependent on the deformation processing history. The activation volume due to non-conservative motion of jogs cannot be lower than $10^2 b^3$ because the density of jogs reaches the saturation through annihilation of vacancy-producing jogs and interstitial-producing jogs. Therefore, non-conservative-motion of jogs is not the rate-controlling mechanism for Zircaloy tubes of the present study.

In 1976, on the basis of the experimental result that oxygen atoms affect the temperature dependence of the flow stress in zirconium, Ramanswami and Craig [20] suggested that the most probable rate controlling mechanism in the temperature range of 300–520 K was the overcoming of impurity atoms (the discrete obstacle model [21]). However, the oxygen content of the stress-relieved Zircaloy tubes is not much different from the annealed Zircaloy and the smaller activation volume in

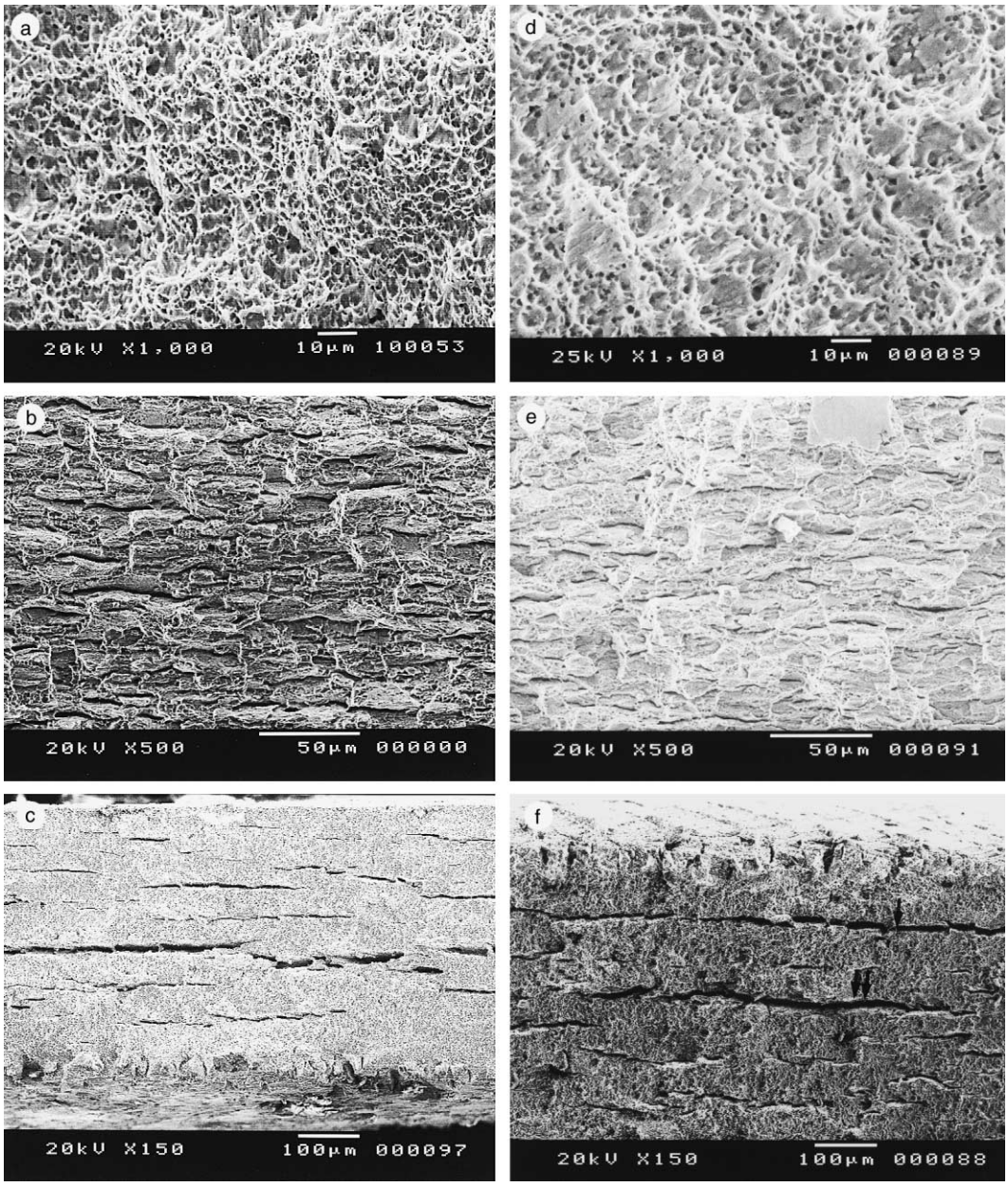

Fig. 6. Fracture surfaces of as-received (a, d) and hydrided (b, c, e, f) R-type (a, b, c) and L-type (d, e, f) Zircaloy tubes. Air cooled (b, e) and furnace cooled (c, f) tubes.

the stress relieved alloy cannot be explained only by overcoming of oxygen atoms. Furthermore, many investigators [22–25] suggested that, based on thermal activation analyses, the discrete obstacle model cannot be responsible for solution strengthening of most alloys. Therefore, the most probable rate-controlling mechanism of Zircaloy tubes appears to be the intersection of dislocations. It was reported by Song et al. [22] that the dislocation density in a commercial stress relieved Zircaloy-4 tubes was $= 2 \times 10^{-11}$ cm^{-2}. The spacing between forest dislocation, λ, was calculated to be 2.24×10^{-8} cm ($= 70b$) based on the observed dislocation density ($\rho = 2 \times 10^{-11}$ cm^{-2}), assuming $\lambda = 1/\sqrt{\rho}$. The activation volume ($70b^3$) calculated based on the observed dislocation density is larger than the observed activation volume (30–$50b^3$). The dislocation density should be larger than 4×10^{11} cm^{-2} to make the spacing between forest dislocation smaller than $50b$. The differ-

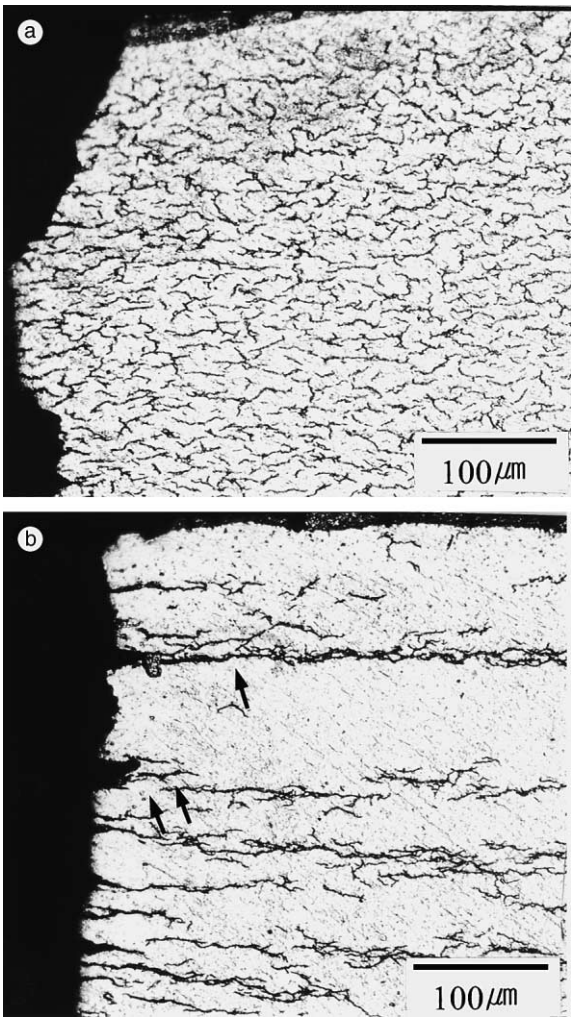

Fig. 7. Transverse sections of the air-cooled (a) and furnace-cooled (b) L-type tubes after fracture.

ence between the predicted activation length (70*b*) and the observed activation length (30–50*b*) may be associated with the role of alloying elements [23,25,26].

Kocks suggested that the activation length (described as 'bulge length' in the paper of Kocks [23]) is affected by the segregated alloying elements although the maximum bulge length is limited by the forest spacing λ (Fig. 21 of Ref. [23]). The interaction between strain hardening and solution hardening, including strain aging, all observed in Zr base alloys can be easily explained by the model of Kocks [23]. Kocks [23] suggested that the segregation of solute atoms at dislocations makes a great contribution to solution strengthening even below the temperature range of dynamic strain aging. Dislocations can collect a significant number of solute atoms from its surroundings after being stopped by forest dislocations [23,25] at low temperatures. Indeed, Hong and Laird [25] and Kocks [23] suggested the similarity between the solution strengthening behavior at low temperatures and the dynamic strain aging behavior at intermediate temperatures. It is well known that the dynamic strain aging at intermediate temperatures in zirconium alloys is caused by the interaction of dislocations and oxygen atoms [3–5]. The element which can be segregated on the dislocations and affects the thermally activation process at low temperatures is thought to be oxygen atoms. Oxygen atoms can segregate easily at dislocations (even at room temperature) while dislocations wait for thermal activation after being stopped at forest dislocations and can contribute to solution strengthening [23,25].

4. Conclusions

On the basis of the present investigation of the effect of circumferential hydrides on the deformation and fracture of Zircaloy tubes, the following conclusions can be drawn.

1. The distribution and size of hydrides were greatly influenced by the cooling rate. Hydride platelets were rather homogeneously distributed in air-cooled tubes whereas they were grouped into long bands in furnace-cooled tubes. Hydrides preferentially precipitated along the interface between the outer layer and the matrix in furnace-cooled L-type tubes.
2. Zircaloy tubes can be slightly strengthened by circumferential hydrides, but the ductility decreased slightly after the formation of circumferential hydrides. In both R-type and L-type tubes, the ductility of air-cooled tubes is greater than that of furnace-cooled tubes, implying that the segregated long hydrides are more detrimental to the ductility although they were circumferentially oriented.
3. The activation volume and, therefore, the deformation mechanism are not appreciably modified by the presence of circumferential hydrides. The similarity of the stress–strain curves before and after hydride formation strongly supports that circumferential hydrides have no appreciable effect on the rate-controlling mechanism.
4. The rate-controlling mechanism of the deformation can be explained by the dislocation intersection mechanism in which the segregation of alloying elements on dislocations affect the activation length.

References

[1] B. Cox, Y.M. Wong, J. Nucl. Mater. 270 (1999) 134.
[2] J.B. Bai, N. Ji, D. Gilbon, C. Prioul, D. Francois, Metall. Mater. Trans. 25A (1994) 1199.

[3] S.I. Hong, W.S. Ryu, C.S. Rim, J. Nucl. Mater. 120 (1984) 1.
[4] S.I. Hong, W.S. Ryu, C.S. Rim, J. Nucl. Mater. 116 (1983) 314.
[5] J.L. Derep, S. Ibrahim, R. Rouby, G. Fantozzi, Acta Metall. 28 (1980) 607.
[6] K.W. Lee, S.K. Kim, K.T. Kim, S.I. Hong, J. Nucl. Mater. 295 (2001) 21.
[7] B.A. Cheaddle, Physical Metallurgy of Zirconium Alloys, CRNL Report, CRNL-1208, 1974.
[8] Y. Choi, J.W. Lee, Y.W. Lee, S.I. Hong, J. Nucl. Mater. 256 (1998) 124.
[9] F. Garzarolli, R.V. Jan, H. Stehle, At. Energ. Rev. 17 (1979) 31.
[10] L.G. Bell, R.G. Duncan, AECL Report, AECL-5110, 1975.
[11] K. Takeda, H. Anada, in: Zirconium in the Nuclear Industry, 12th Int. Symposium, ASTM STP, vol. 1354, 2000, p. 592.
[12] J.S. Kim, S.Y. Park, M.H. Lee, Y.H. Jeong, Y.H. Jung, Korean J. Mater. Res. 9 (1999) 978.
[13] A. Sawatzky, J. Nucl. Mater. 2 (1962) 62.
[14] D.D. Himbeault, C.K. Chow, M.P. Puls, Metall. Trans. 25A (1994) 135.
[15] R.P. Marshall, M.R. Louthan, Trans. ASM 56 (1963) 693.
[16] H. Conrad, J. Met. 16 (1964) 582.
[17] M.J. Luton, J.J. Jonas, Can. Met. Quart. 11 (1972) 79.
[18] S.I. Hong, G.T. Gray III, J.J. Lewandowski, Acta Metall. Mater. 41 (1993) 2337.
[19] S.I. Hong, G.T. Gray III, J. Mater. Sci. 29 (1994) 2987.
[20] B. Ramaswami, G.B. Craig, Trans. AIME 239 (1967) 1226.
[21] P. Haasen, in: T.B. Massalski (Ed.), Alloying Behavior and Effects in Concentrated Solid Solutions, Gordon and Breach, London, 1965, p. 270.
[22] J.S. Song, S.D. Kim, S.I. Hong, Y. Choi, J.W. Kim, J. Korean Inst. Metall. Mater. 35 (1997) 1668.
[23] U.F. Kocks, Metall. Trans. 16A (1985) 2109.
[24] Z.S. Basinski, R.A. Foxall, R. Pascual, Scripta Metall. 6 (1972) 807.
[25] S.I. Hong, C. Laird, Acta Metall. Mater. 38 (1990) 1581.
[26] S.I. Hong, Scripta Mater. 44 (2001) 995.